

Article

Not peer-reviewed version

---

# Advanced Delivery of Curcumin and Nicotinamide: Promising Solutions for Skin Infections and Melanoma

---

Omar Markab , [Zainab Lafi](#)\*, Naeem Shalan , Hala Al Daghistani , Ali Fahadawi , Razan Madi

Posted Date: 23 September 2024

doi: 10.20944/preprints202408.1541.v2

Keywords: Natural compounds; melanoma; skin infection; synergism; liposomes



Preprints.org is a free multidiscipline platform providing preprint service that is dedicated to making early versions of research outputs permanently available and citable. Preprints posted at Preprints.org appear in Web of Science, Crossref, Google Scholar, Scilit, Europe PMC.

Copyright: This is an open access article distributed under the Creative Commons Attribution License which permits unrestricted use, distribution, and reproduction in any medium, provided the original work is properly cited.

Article

# Advanced Delivery of Curcumin and Nicotinamide: Promising Solutions for Skin Infections and Melanoma

Omar Markab, Zainab Lafi \*, Naeem Shalan, Hala. Al Daghistani, Ali Fahdawi and Razan Madi

Pharmacological and Diagnostic Research Center, Faculty of Pharmacy, Al-Ahliyya Amman University

\* Correspondence: z.lafi@ammanu.edu.jo; Phone: (+962)795857853

**Abstract:** The interest in natural remedies in modern medicine has revealed potent disease-fighting agents, such as Curcumin (CUR) and nicotinamide (NIC), known for their antioxidant, anti-inflammatory, and immune-boosting properties. This study explores the antibacterial and antimelanoma potential of a CUR-NIC combination and its liposomal formulation. The antibacterial efficacy was assessed against skin infection-causing bacteria, *Staphylococcus aureus*, while cytotoxicity and migration assays were conducted on the melanoma B16 cancer cell line. The CUR-NIC combination (1:1) demonstrated an inhibition zone of  $18 \pm 0.8$  mm against *S. aureus* and a MIC of  $31.25 \mu\text{g/ml}$ , outperforming CUR alone. Whereas Lip-CUR-NIC showed an inhibition zone of  $12 \pm 0.8$  mm against *S. aureus* and a MIC of  $37.5 \mu\text{g/ml}$ . Notably, the cytotoxicity assay revealed that the CUR-NIC duo synergistically inhibited melanoma cell proliferation ( $CI < 1$ ). Liposomal preparations further enhanced this effect, with Lip-CUR-NIC showing a remarkably low  $IC_{50}$  of  $8.5 \pm 0.3 \mu\text{M}$  compared to CUR ( $IC_{50} = 9.8 \pm 2.2 \mu\text{M}$ ) and NIC ( $IC_{50} = 135.95 \pm 10.2 \mu\text{M}$ ). These findings highlight the synergistic potential of CUR and NIC, especially in their liposomal form, offering a promising strategy for more effective cancer treatment.

**Keywords:** natural compounds; melanoma; skin infection; synergism; liposomes

## 1. Introduction

The discovery of bioactive compounds and vitamins in natural nutrients has led to significant advancements in medicine due to their diverse biological activities, including anti-inflammatory, antioxidant, antimicrobial, and anticancer effects. These compounds play vital roles in maintaining health by supporting various physiological functions, such as regulatory and catalytic activities [1–5].

However, the increasing threat of antibiotic resistance presents a major global health crisis. This phenomenon occurs when bacteria develop mechanisms to evade the effects of antibiotics, rendering these drugs ineffective. The misuse and overuse of antibiotics have accelerated the emergence of resistant strains, making infections harder to treat. Compounding the issue is the slow pace of new antibiotic development, raising concerns about a future where common infections could once again become deadly [6,7]. Simultaneously, melanoma, a severe form of skin cancer originating from melanocytes, remains a critical public health challenge. Exposure to ultraviolet (UV) radiation is a primary risk factor for melanoma. Despite the effectiveness of current chemotherapies, their use is often limited by significant systemic toxicity and the emergence of multidrug-resistant (MDR) cancer cells [9,10]. Given these limitations, there is a growing interest in exploring safer and more effective treatment strategies, particularly those involving natural compounds with known therapeutic properties [8]. Exposure to ultraviolet (UV) radiation from the sun or tanning beds is a significant risk factor for melanoma. Despite the success of chemotherapies, they result in systemic toxicity and the eventual emergence of multi-drug resistant (MDR) cancer cells [9].

CUR, a natural compound with strong antioxidant and anti-inflammatory properties, has garnered attention for its potential role in cancer prevention and treatment. By mitigating oxidative stress and chronic inflammation—two key contributors to tumorigenesis—CUR may inhibit tumor

initiation and progression [13,14]. Nicotinamide (NIC), another promising agent, enhances DNA repair through the activation of Poly-ADP-ribose Polymerase (PARP), thereby increasing the sensitivity of cancer cells to DNA-damaging treatments such as radiation and certain chemotherapeutic drugs [10,11]. Several studies have investigated the antibacterial activity of NIC against many strains such as methicillin-resistant *Staphylococcus aureus* (MRSA) [12], *Mycobacterium tuberculosis* and Bacille Calmette-Guérin [13,14].

NIC exhibits distinct mechanisms of action that contribute to its potential as an anticancer agent, as supported by scientific evidence [15–17]. One notable mechanism involves its involvement in DNA repair processes. Nicotinamide enhances the capacity for DNA repair by activating Poly-ADP-ribose Polymerase (PARP), an enzyme critical for the restoration of DNA damage [18,19]. This particular property enables NIC to effectively sensitize cancer cells to DNA-damaging agents, including radiation and specific Chemotherapeutic Drugs [19]. Nanotechnology reaching new heights, many researchers are driven to create a safer and more efficient medication delivery approach for cancer treatment. Recently many approved anticancer medications are derived from natural substances. Liposomal formulations provide significant advantages for drug delivery, particularly by improving the stability and bioavailability of drugs like curcumin, which typically suffers from poor absorption and rapid degradation. Encapsulating compounds with different solubility profiles in liposomes as a combination enhances their ability to target bacteria more effectively, while also addressing solubility and stability challenges. Although our main focus was on their antibacterial effects, we believe that investigating liposomal formulations is essential for optimizing the therapeutic potential of these compounds [20,21]. Given the overlapping challenges of antibiotic resistance and melanoma, this study aims to explore the combined use of CUR and NIC in a liposomal formulation as a dual-therapeutic approach. The simultaneous investigation of these two conditions is justified by the potential for CUR and NIC to exert synergistic effects against both bacterial infections and cancer. The liposomal delivery system, prepared using the ethanol injection method, is expected to enhance the skin penetration and therapeutic efficacy of CUR and NIC, making this combination a promising candidate for adjuvant treatment in skin infections and melanoma.

## 2. Material and Methods

Nicotinamide (NIC) was obtained from Sigma-Aldrich (USA), CUR (CUR) was obtained from ICT (Japan). 1,2-dipalmitoyl-*sn*-glycero-3-phosphocholine (DPPC) was obtained from Avanti Polar Lipids, Inc. (Alabaster, Alabama, USA) and Cholesterol (CHO) was obtained from Carbosynth (UK). Phosphate Buffer Saline (PBS) was purchased from LONZA® (USA). PLC grade Methanol was from Sigma-Aldrich (USA). HPLC-grade Ethanol was from the carbon group- England. All chemicals and solvents were of high purity.

### 2.1. Liposomal Preparation

Liposomes of CUR and NIC were prepared using the conventional ethanol injection technique as described in our previous article (Fahdawi et.al. 2024). Briefly, 10 mg of DPPC, CHO 2.5 mg, and 2.0 mg CUR were dissolved in ethanol, which was then warmed at 40 °C water bath. NIC 2mg/ml was dissolved in PBS and heated using hot plate at ~50 °C with string 700 rpm. Then the warm drug lipid ethanol mixture was injected rapidly into the PBS with heating and continuous stirring. After were prepped, the free of CUR and NIC were removed and washed and stored at 4°C [22]. The average particle size, Zeta Potential (charge) and Polydispersity Index (PDI) for liposomes were measured by DLS experiments using Zetasizer, Nano-ZS (Malvern Instruments Ltd., Malvern, UK). The Stability of the loaded liposomes was performed at 4 °C with storage times of one month. The EE % of CUR and NIC into liposomes was expressed as the percentage of drug complex encapsulated inside liposomes [23,24].

### 2.2. Screening of the Antibacterial Activity

#### 2.2.1. Agar Well-Diffusion Method

The Antibacterial activity screening was performed by the agar well-diffusion method according to guidelines of the Clinical and Laboratory Standards Institute. Muller-Hinton Agar Plates were prepared according to the manufacturer instructions (Thermo Fisher Scientific, Waltham, MA, USA). Wells were made into the agar using a 6 mm diameter sterile borer. The selected bacteria were mainly *S. aureus* and *p. aeruginosa* (ATCC® 29213). Bacterial cultures were started in Muller-Hinton (MH) broth, and incubated overnight in the shaker at 37° C. Before use, the inoculum turbidity was standardized at OD<sub>520 nm</sub> = 0.1 (contrasted to 0.5 M McFarland). Bacteria were swabbed uniformly on the agar plates using sterile cotton applicators dipped into the standardized inoculum. Each well had 100 µL of the desired drug and liposomes concentration, while the control well contained the same volume of DMSO. Plates were then incubated at 37°C for 24 h, and the diameter of the inhibition zones was measured in millimeters (mm). Data are presented as the means for readings obtained from three different wells for each concentration.

### 2.2.2. Minimum Inhibitory Concentration (MIC)

If the bacteria were inhibited by the 1000 µg/mL at the primary screening, a determination for the MIC will take place using two-fold lower concentrations starting from 500, 250, 125, and 62.5 µg/ml. Five wells were made into the agar before streaking the plates with a standardized bacterial inoculum. Each well was filled with 100 µL of a selected drug, liposomes or with a control solvent which was used to solubilize the drugs and liposomes (DMSO or PBS). The plates were then incubated at 37°C for 24 h, and the inhibition zones were measured in mm.

### 2.2.3. *S. aureus* Susceptibility

The antibacterial activity of free Antibiotics and CUR and NIC loaded liposomes were evaluated by the broth Microdilution Method, according to guidelines of the Clinical and Laboratory Standards Institute [25], followed by turbidity evaluation. Briefly, the formulations were diluted in PBS to produce a serial dilution with concentrations ranging from: 0.1875 to 200 µg/mL of both drugs and their liposomes. Bacterial Suspensions were performed from a MSSA overnight culture diluted in broth media until reaching a value of 0.5 in a McFarland scale equivalent to 10<sup>8</sup> colony forming unit/ml by measuring the optical density at 600 nm. Bacterial Suspension was cultured in 96-well cell culture plates at 5 × 10<sup>5</sup> bacterial density and incubated with the Antibiotics or the formulations, at 37 °C during 24 h. A negative control containing a Suspension of bacteria in broth, without treatment, and a sterile control containing broth only without bacteria, were included. Minimum Inhibitory Concentration (MIC: the lowest Antibiotic concentration able to prevent visible bacterial growth, resulting in the absence of turbidity) was determined Spectrophotometrically, at 570 nm in a microplate reader (Bio-Rad laboratories, Inc., Hercules, CA, USA).

## 2.3. Cell Culture

The B16 mouse cancer cell line was obtained from the American Type Culture Collection (ATCC, Manassas, VA, USA). These cells were cultivated as attached monolayers and preserved in DMEM medium (EuroClone, Italy), enriched with 10% (v/v) heat-inactivated Fetal Bovine Serum (FBS) (Euro Clone, Italy), 1% Penicillin-Streptomycin (Euro Clone, Italy), and 2 mM L-glutamine. Incubation of the cells was carried out at 37°C within a Tissue Culture Incubator (Memmert, Schwabach, Germany) containing 5% CO<sub>2</sub>.

### 2.3.1. Cell Viability Assay (MTT)

An MTT Assay was conducted to determine the IC<sub>50</sub> of (Lip-CUR, Lip-NIC and their co-loaded liposome (Lip-CUR-NIC) prepared by the Ethanol Injection Technique on cancer cells. Roughly, (5 × 10<sup>3</sup> cells/well) of B16 mouse Melanoma cancer cells placed into a 96-well plate (Corning, USA). Cells were subjected to concentrations ranging from 3.125 to 200 µM.

Briefly, the different concentrations were prepared as follows; 200 µL of each Liposomal formulation (Lip-CUR, Lip-NIC and Lip-CUR-NIC) was mixed with 800 µL media to get a final

volume of 1 ml Stock Solution (200  $\mu\text{M}$ ) for each formulation. Serial dilutions were made for each Stock Solution where 500  $\mu\text{L}$  of each Stock Solution was diluted with 500  $\mu\text{L}$  media. Then, the cells were cultured at 37  $^{\circ}\text{C}$  in a 5%  $\text{CO}_2$  Incubator for 72 hours. Afterward, the previous media was removed, and 100  $\mu\text{L}$  of fresh media containing MTT Assay Salt (Bioworld, USA) was added to each well. Subsequently, the plates were incubated at 37  $^{\circ}\text{C}$  for 3 hours, followed by the addition of 50  $\mu\text{L}$  of Solubilization Solution (DMSO) to each well to assess Viability. The optical absorbance of the Solution was measured at 560 nm using ELIZA Plate Reader (USA).

### 2.3.2. Cell Migration Assay

Melanoma B16 cell line was seeded in sterile 6-well cell culture plates at a density of 800,000 cells per well and then incubated for 24 hours at 37 $^{\circ}\text{C}$  with 5%  $\text{CO}_2$ . The following day, a vertical scratch was created at the center of the cell's monolayer using a sterile 1,000  $\mu\text{L}$  micropipette tip for either free drugs or nanoliposome's treatment. Subsequently, each well was washed twice with sterile PBS. After 1 day, cells were exposed to CUR, NIC CUR-NIC and Lip-CUR-NIC at three different concentrations near  $\text{IC}_{50}$ , as determined by the MTT test. Finally, images of the scratches were captured before and during cell treatment using a phase contrast microscope (model P. MICRO-001, Nikon) equipped with a 4 $\times$  magnification objective. The Images J software was employed to calculate the wound closure area ( $\mu\text{m}^2$ ). DMSO and free media served as negative controls. The wound closure rate was observed on day 1 (before treatment) and day 2 after 48h of cell therapy [26]. Empty liposomes and media were employed as a negative control.

The wound closure (%) was calculated using eq

$$\text{Rate of wound closure (\%)} = \frac{\text{Area for day1} - \text{Area for day 4}}{\text{Area for day1}} \times 100$$

### 2.4. DPPH Assay

The free radical scavenging activities of four treatments—Vitamin C, NIC, CUR, and CUR-NIC—prepared using the Ethanol Injection Technique, were evaluated using the 2,2-diphenyl-1-picrylhydrazyl (DPPH) free radical scavenging assay, following the method described by Shirazi et al. (2014). For the calibration curve, a stock solution of Vitamin C was prepared by dissolving 1 mg in 1 mL of methanol to create standard stock solutions of Vitamin C, CUR, NIC, and CUR-NIC. Serial dilutions were made by mixing 500  $\mu\text{L}$  of each sample with 500  $\mu\text{L}$  of methanol. The DPPH solution was prepared by dissolving 8 mg of DPPH in 10 mL of methanol, producing a deep violet-colored solution. In a 96-well plate, 100  $\mu\text{L}$  of each sample was combined with 100  $\mu\text{L}$  of the freshly prepared DPPH solution. Each assay was performed in triplicate and incubated in the dark for 30 minutes. Controls included DPPH and CUR in methanol. Absorbance was then measured at 517 nm using an ELISA plate reader. The Vitamin C calibration curve was used to calculate both the percentage of free radical inhibition and the concentration of Vitamin C, CUR, NIC, and CUR-NIC formulations required to achieve 50% free radical inhibition ( $\text{IC}_{50}$ ).

$$\text{(\% Inhibition of Free Radical)} = (\text{Ab Control} - \text{Ab Sample}) / \text{Ab Control} * 100$$

%

### 2.5. Statistical Analysis

The findings were expressed as the mean  $\pm$  standard deviation from a minimum of three separate trials. GraphPad Prism 8 (GraphPad Software Inc., USA), CompuSyn.exe (Version 1) and Microsoft Office Excel (Microsoft, USA).

## 3. Results and Discussion

### 3.1. Liposomal Preparation and Characterization

The liposomal formulation of Lip-CUR-NIC was developed and fully characterized using UV spectrophotometry and HPLC analysis, as previously reported by Fahdawi et al. (2024). In this study, the Lip-CUR-NIC formulation was biologically evaluated alongside the pure compounds CUR and NIC. The average particle size for all preparations was under 200 nm (Figure 1A), and the particle size distribution was assessed using the polydispersity index (PDI). A lower PDI indicates a more uniform size distribution, with values below 0.4 considered good for monodispersed nanoparticles (Figure 1B) (Bellone et al., 2015). The stability of the liposomal formulations was monitored over 30 days, focusing on size distribution (Figure 1C) and zeta potential (Figures 1D, 1E). These parameters, including average diameter, PDI, surface charge, encapsulation efficiency (EE%), and loading efficiency (LE%), were consistent with those reported in the previous study for the same liposomal formulations (Fahdawi et al., 2024). Additionally, the *in vitro* release profiles of CUR and NIC were evaluated over 72 hours, showing that CUR had a slower release from the Lip-CUR-NIC formulation compared to NIC. This difference is likely due to the higher solubility of NIC in PBS compared to CUR.

The release profiles of CUR and NIC from the Lip-CUR-NIC show distinct differences, with CUR exhibiting a faster and higher cumulative release compared to NIC. CUR's profile indicates an initial burst followed by a sustained release, while NIC demonstrates a slower, more controlled release throughout the study. This difference is likely due to the varying interactions of the two compounds with the [27,28]

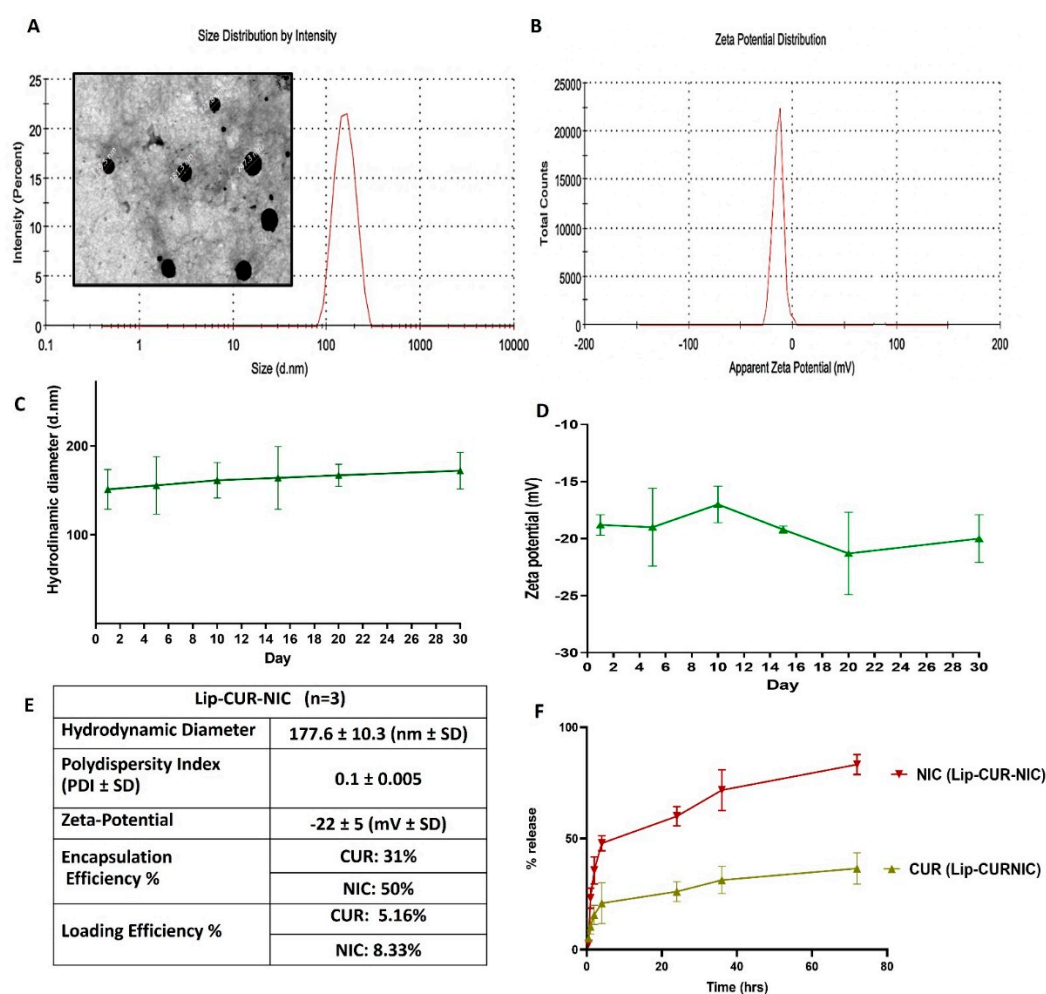


**Figure 1.** Characterization of the prepared liposomes A) Size Distribution and morphology of particles from TEM image B) Average Zeta Potential C) Stability Test for liposomal Hydrodynamic Diameter for one month D) Stability Test for liposomal Zeta Potential for one month E) Summary

table for average size, zeta potential, encapsulation and loading efficiency F) *In vitro* release assay for CUR and NIC from Lip-CUR-NIC (mean  $\pm$  SD, n = 3).

### 3.2. Antioxidant Activity and DPPH Assay

A DPPH assay, which measures the free radical scavenging activity of CUR, NIC, CUR- NIC and Vit C as a standard (Figure 2A, 2B). The assay results are plotted as percentage inhibition of the DPPH radical against the concentration of the tested substances in mg/ml. NIC exhibited the lowest activity among the tested samples, with a more gradual increase in inhibition percentage as the concentration increases, while CUR demonstrated higher activity than NIC, with a steeper curve that approaches the activity level of Vit C at higher concentrations. The combination of CUR and NIC showed an improved scavenging effect compared to NIC alone and slightly better than CUR alone, suggesting a potential synergistic effect between the two on radical scavenging activity. As expected, Vitamin C exhibited the highest radical scavenging activity, nearing 100% inhibition, since it is a well-known potent antioxidant used as the positive control in the assay.

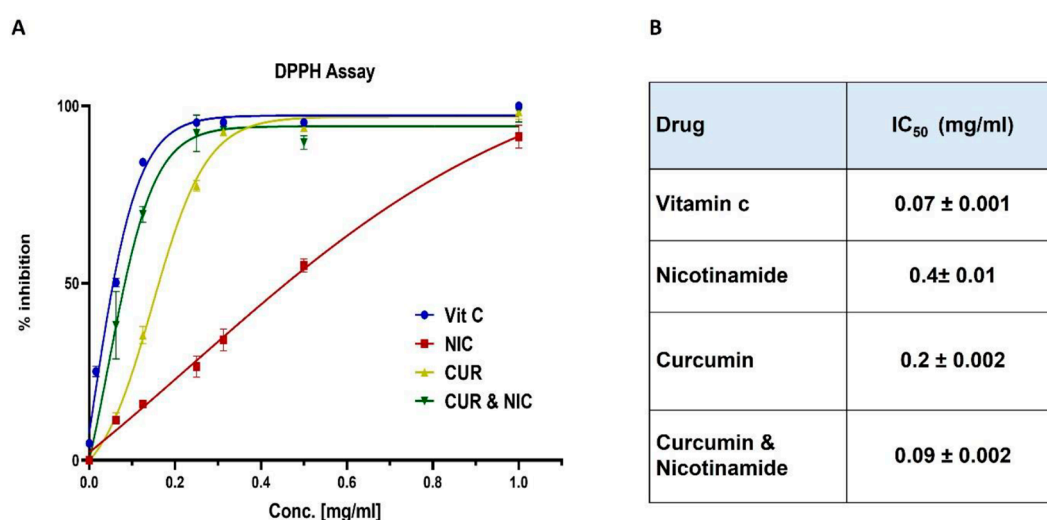


**Figure 2.** A) Percent Inhibition of DPPH free radical using CUR, NIC and their combination B) IC<sub>50</sub> of DPPH radical CUR, NIC, CUR-NIC and lip-CUR-NIC (mean  $\pm$ SD, and n=3).

### 3.3. Antibacterial Activity of CUR, NIC and lip- CUR-NC

An initial assessment of the antibacterial activity of CUR, NIC, and their combination CUR-NIC, along with their respective liposomal formulations, against *S. aureus* and *S. epidermidis* is shown in Figures 3A, 3B, 3C, and 3D. CUR demonstrated effective inhibition of *S. aureus* growth, while NIC alone, at various concentrations, did not show significant antibacterial activity. However, when NIC was combined with CUR, it enhanced CUR's antibacterial effect. These findings indicate that the antibacterial activity of the CUR-NIC combination is concentration-dependent (Figure 3), highlighting a potential synergistic interaction between the two compounds.

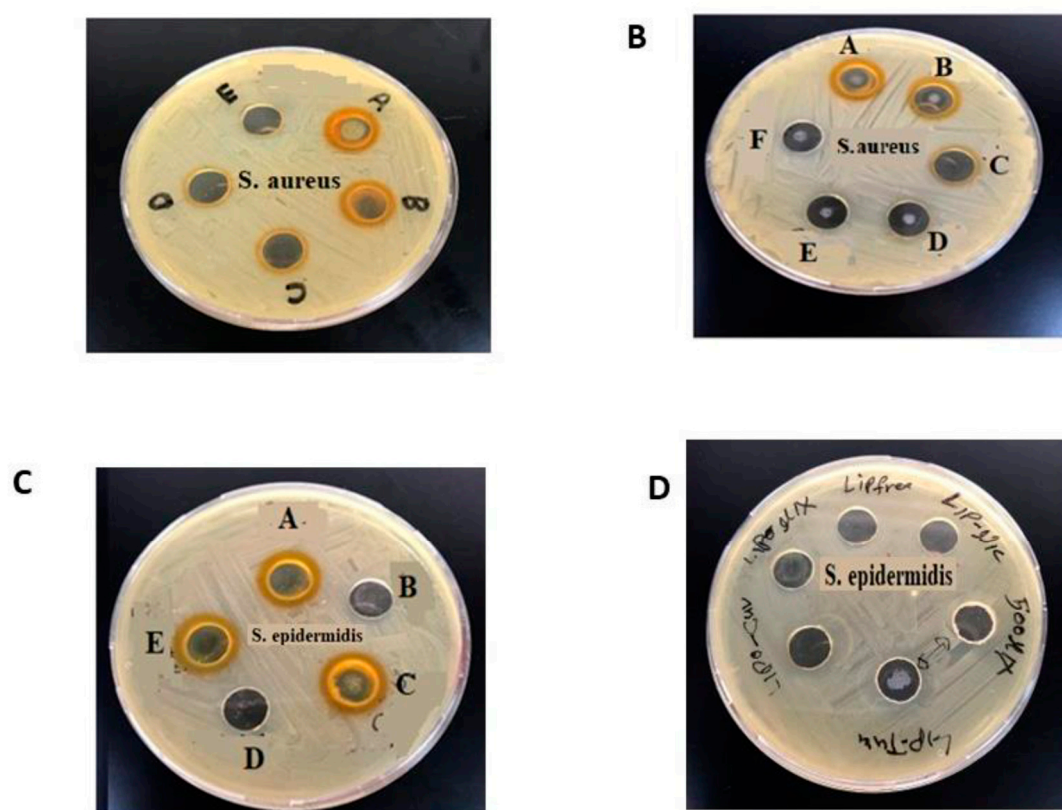


**Figure 3.** Screening of antibacterial activity by well-Diffusion method A) CUR-NIC demonstrated moderate inhibition zone against *S. aureus* across of four serial dilutions (1000, 125, 62.5, and 31.5  $\mu\text{g/ml}$ ). B) The Lip-CUR-NIC tested across six serial dilutions (1000, 250, 125, 62.5 and 31.5  $\mu\text{g/ml}$ ), also showed notable inhibition against *S. aureus*. C) Screening of CUR (A), NIC (B), CUR-NIC (C) and Lip-CUR-NIC (E) against *S. epidermidis*. D) The liposomal formulations showed no activity against *S. epidermidis*.

When evaluating the antibacterial activity of CUR, CUR-NIC, Lip-CUR, and Lip-CUR-NIC across concentrations ranging from 3.13 to 400  $\mu\text{g/ml}$ , CUR exhibited an MIC of 62.5  $\mu\text{g/ml}$ , while Lip-CUR showed a slightly lower MIC of 75.5  $\mu\text{g/ml}$ . This suggests that the liposomal formulation of CUR does not significantly improve its antibacterial efficacy against *S. aureus*. Similarly, CUR-NIC had an MIC of 31.25  $\mu\text{g/ml}$ , whereas Lip-CUR-NIC displayed an MIC of 37.7  $\mu\text{g/ml}$  at the same concentrations (Figure 4A, 4B), indicating a comparable trend between the free and liposomal formulations.

A							B		
Conc $\mu\text{g/ml}$	Control	CUR	Lip-CUR	CUR-NIC	Lip-CUR-NIC	NIC	Antibiotic (n=2)	Inhibition Zone diameter mm	MIC
400							Erythromycin (sensitive bacteria)	26	-
200							Vancomycin (Moderately sensitive)	10	-
100							Vancomycin (Resistant bacteria)	0	-
50							CUR	16 $\pm$ 0.85	62.5 $\mu\text{g/ml}$
25							NIC	0	1.5 mg/ml
12.5							CUR-NIC	18 $\pm$ 0.8	31.25 $\mu\text{g/ml}$
6.25							Lip- Free	0	-
3.13							Lip-NIC	0	-
							Lip- CUR	10 $\pm$ 0.3	75.5 $\mu\text{g/ml}$
							Lip-NIC-CUR	12 $\pm$ 0.9	37.7 $\mu\text{g/ml}$

**Figure 4.** A) Plate titer method for *S. Aureus* Susceptibility Test using CUR, Lip-CUR, CUR-NIC, Lip-CUR-NIC and NIC, at a concentration range of (400-3.13  $\mu\text{g/ml}$ ) B) Table of inhibition zone and MIC of the CUR, Lip-CUR, CUR-NIC, Lip-CUR-NIC and NIC.

As noted by Harush-Frenkel in 2010, positively charged nanoparticles were associated with increased side effects and toxicity. In contrast, the prepared liposomes in this study exhibited a negative average zeta potential, which is more favorable for their safety profile. [29].

Inhibitors of bacterial resistance present promising treatment options for patients with antibiotic-resistant infections. The use of natural inhibitors could enhance the effectiveness of retreatment in patients who previously received ineffective antibiotics and help prevent the emergence of new antibiotic-resistant bacterial strains. Various studies have consistently demonstrated that CUR exhibits antimicrobial effects, with no contradictory findings reported on this topic [30,31].

Teow and Ali (2015) conducted a study to examine the combined antibacterial effects of CUR and eight different antibiotic groups. Using disc diffusion assays, they found synergistic effects between CUR and most of the antibiotics against *S. aureus*. However, in microdilution assays, synergy was only observed with three antibiotics: ciprofloxacin, gentamicin, and amikacin. The other tested antibiotics showed no significant interaction, though no antagonism was detected. These findings align with this study, likely due to the use of similar experimental methods. [32].

The antibacterial activity of CUR was evaluated using the broth microdilution method, checkerboard dilution test, and time-kill assay. CUR demonstrated antimicrobial activity against all tested strains. In the checkerboard test, CUR significantly reduced the MIC of antibiotics such as oxacillin, ampicillin, ciprofloxacin, and norfloxacin, which are commonly used to treat methicillin-resistant *Staphylococcus aureus* (MRSA)[33].

Like this study, Zhou et al. demonstrated that the combined treatment of CUR and Erythromycin effectively suppressed bacterial growth and alleviated bone infection. The combination showed stronger efficacy against MRSA-induced osteomyelitis in rats compared to monotherapy [34].

In a different study, Wang et al. utilized CUR as a natural antibacterial and antifungal Agent against various foodborne pathogens, including *Staphylococcus Aureus*, *Escherichia coli*, *Yersinia enterocolitica*, *Bacillus cereus*, and *Aspergillus niger*. They improved the stability and solubility of CUR by using Microcapsules. The study demonstrated a broad-spectrum inhibitory effect of CUR against all tested organisms using the Oxford Cup Method. The results also indicated that CUR had greater antibacterial activity against Gram-positive bacteria than Gram-negative bacteria, while its Antifungal Activity was significantly higher than its antibacterial activity [35].

Gunes et al. investigated the effect of CUR on standard bacterial strains at high concentrations and demonstrated its strong antibacterial activity at high doses on animals. This study was conducted in Turkey, and the similarity in results could be attributed to the potential presence of the same bacterial strains and resistance genes [36].

In a study conducted by Shailendiran et al. in 2011, the antibacterial properties of CUR and non-formulated CUR were examined against both a gram-positive bacterial strain (Cocci) and a gram-negative bacterial strain such as *E. coli*. The study applied the agar disc assay to observe the size of the inhibition zone over time. Results showed that after 10 hours, a clearly visible inhibition zone was observed, indicating inhibition of bacterial growth. However, this zone became less distinct after 24 hours for both CUR and nanocurcumin-treated discs. These findings suggest that the tested samples exhibited bacteriostatic properties, inhibiting bacterial growth rather than killing the bacteria outright [37]. In another study conducted by Hu et al., the antimicrobial activity of CUR against *S. Mutans* was examined, and the inhibitory ability of CUR on purified Sortase A was evaluated using Western blot and Real-time PCR. The study revealed that CUR can effectively inhibit purified *S. Mutans* Sortase A at a concentration equivalent to half of the minimum inhibitory concentration (MIC), leading to a reduction in *S. Mutans* biofilm formation [38].

Furthermore, Lzui et al. demonstrated that CUR exhibited a dose-dependent inhibition of the growth of *Prevotella intermedia*, *P. gingivalis*, *Treponema denticola*, and *Fusobacterium nucleatum*. Even at very low concentrations, CUR significantly suppressed bacterial development [39].

Additionally, testing the liposomal formulations against *Staphylococcus epidermidis*, a key component of the skin's normal flora, revealed that CUR alone inhibited bacterial growth. This raises concerns about CUR's selectivity for pathogenic bacteria versus beneficial bacteria and highlights the need to assess the safety of such formulations in clinical applications. While CUR shows promise as an antibacterial agent, its impact on normal skin flora could affect skin health, suggesting further investigation is needed to balance therapeutic efficacy with the preservation of healthy microbiota.

### 3.4. Cytotoxicity Study and Anticancer Activity

When assessing the anticancer potential of CUR and NIC, and their combination CUR-NIC, it was found that CUR-NIC had the most significant effect in reducing cancer cell viability, particularly at moderate concentrations. This indicates a possible synergistic effect between CUR and NIC in combating cancer, making their combination a promising candidate for further exploration in cancer therapy. Whereas, in the case of drug-loaded liposomes, encapsulating CUR increased its IC<sub>50</sub> to 50 ± 9.2 μM, demonstrating reduced effectiveness compared to free CUR. NIC, on the other hand, remained relatively ineffective with an IC<sub>50</sub> value still above 200 μM (Figure 5A). When considering the liposomal formulations, CUR had an IC<sub>50</sub> of 31.4 ± 3.2 μM, and NIC exhibited an IC<sub>50</sub> of 190 ± 7.3 μM. These results show that while liposomal CUR and NIC both improved in effectiveness compared to their single-drug liposome counterparts, they were still less effective than the free CUR-NIC combination (Figures 5A and 5B).

The IC<sub>50</sub> values for CUR and NIC, when administered alone and in combination to B16 cells, are shown in Figure 5C. For the free drugs alone, CUR had an IC<sub>50</sub> value of 27.3 ± 2.3 μM, indicating moderate potency. NIC had an IC<sub>50</sub> value exceeding 200 μM, showing low effectiveness as a single agent against B16 cells. When used in combination, the IC<sub>50</sub> for CUR significantly decreased to 9.8 ± 2.2 μM, showing increased potency. Similarly, the IC<sub>50</sub> for NIC dropped to 135.95 ± 10.2 μM, indicating enhanced effectiveness when used with CUR. The isobologram analysis for the CUR-NIC combination (Figure 6A) plots three iso-effective combinations of Dose A (CUR) and Dose B (NIC) corresponding to Fraction Affected (Fa) values of 0.5, 0.75, and 0.9. This analysis shows that either drug alone can achieve a 50% effect at a certain dose, but the combination provides a more potent effect at lower doses.

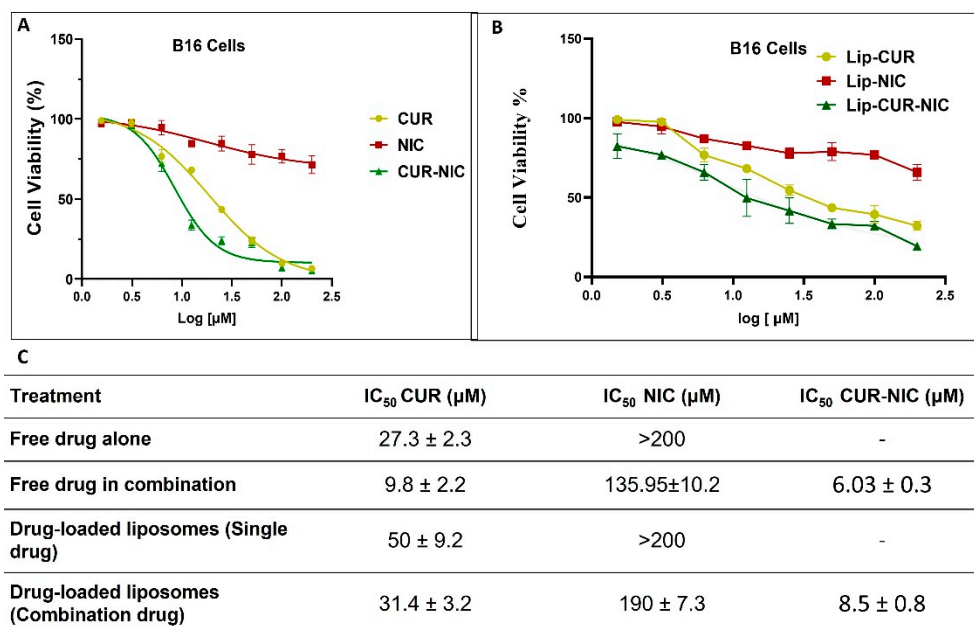


**Figure 5.** (A) The Dose Response Curve for B16 cancer cells treated with Free CUR, NIC and their mixture (0.4-200 μM, n=3) (B) The Dose Response Curve for B16 cancer cells treated with Lip-CUR, Lip-NIC and Lip-CUR-NIC (0.4-200 μM, n=3) (C) Summary of IC<sub>50</sub> values for single and combination of CUR & NIC against B16 cells.

The Isobologram indicates a synergistic interaction between CUR and NIC when combined at a 1:1 ratio, as the combination points fall below the line of additivity. This synergy implies that lower doses of each drug can be used in combination to achieve a high level of effect, potentially reducing side effects, and increasing treatment efficacy, allowing for dose reduction while maintaining or improving therapeutic outcomes.

The Combination Index (CI) plot for the CUR and NIC Free Powder Combination, quantifies the interaction between two drugs, with  $CI < 1$  indicating synergy,  $CI = 1$  indicating an additive effect, and  $CI > 1$  indicating antagonism (Figure 6A, 6B, 6C, 6D, 6E).

The Combination Index (CI) values at various Fraction Affected (Fa) levels, ranging from 0 (no effect) to 1 (complete effect). For the CUR+NIC combination, most CI values fall below 1 across the Fa range, indicating increasing synergy, particularly at higher Fa levels.

Figure 6D illustrates the dose-effect curves for CUR, NIC, and their combination (CUR-NIC), plotting Fa against dose to show the impact on cell viability. CUR exhibits a steep dose-effect relationship, effectively inhibiting cell viability even at low doses and reaching near-complete inhibition (Fa close to 1) at lower doses. In contrast, NIC displays a more gradual dose-effect curve with less inhibition of cell viability, even at higher doses, and does not achieve the same level of inhibition as CUR. The CUR-NIC combination has a dose-effect curve similar to CUR, suggesting that the combination is as effective as CUR alone and that NIC does not negatively impact CUR's inhibitory effect.

The Dose Reduction Index (DRI) quantifies the potential dose reduction in combination therapy compared to using each drug alone. CUR shows a significant increase in DRI with Fa, indicating up to a fivefold or greater dose reduction when used in combination. In contrast, data points for NIC are absent, suggesting NIC does not contribute to dose reduction in the combination. The DRI curve for CUR indicates a strong synergistic interaction, enabling significant dose reduction while maintaining anticancer efficacy. At the highest Fa level (0.97), the DRI for CUR exceeds 100, and for NIC surpasses 200, indicating the doses required to achieve 97% inhibition of cell viability in combination.

The CUR-NIC combination has a notably lower  $IC_{50}$  of 10, a slope of 0.867, and a high correlation coefficient of 0.981, reflecting a potent effect with a well-fitting dose-response curve. When delivered via Lip-CUR and Lip-NIC, Lip-CUR shows moderate anticancer activity with an  $IC_{50}$  of 20, while Lip-NIC has an  $IC_{50}$  above 50. However, Lip-CUR-NIC demonstrates the most significant decline in cancer cell viability among all treatments, highlighting the potential of liposomal delivery to enhance cancer treatment efficacy.

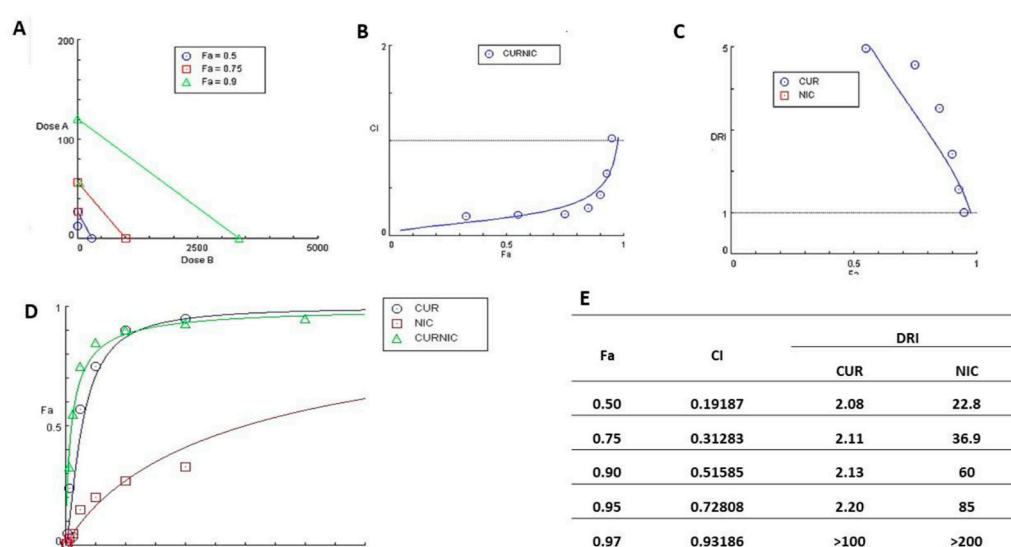


**Figure 6.** (A) Isobologram for combination: CUR-NIC (CUR+NIC [1:1]) (B) Combination Index Plot of CUR and NIC Free Powder (C) Dose-reducing Index Curve of CUR and NIC combination (D) Dose-

effect Curve of CUR and NIC combination (E) Summary of Combination Index (CI) and dose Reducing Index of (DRI) CUR-NIC.

Wang et al. studied curcumin-loaded MPEG-PLA micelles for melanoma treatment, both in lab tests (in vitro) and in animal models (in vivo). They found that the spherical curcumin/MPEG-PLA micelles disperse well in normal saline and provide a sustained release of the drug. These micelles also showed stronger cell-killing effects. Further histochemical analysis in animal studies confirmed their ability to trigger melanoma cell death and block new blood vessel formation in tumors. Their conclusion is that these curcumin/MPEG-PLA micelles hold promise for clinical melanoma treatment.

Fontes et al. explored the combination of CUR and disulfiram for treating B16 melanoma cells. Their research, both in vitro and in vivo, showed that combining CUR and disulfiram had a synergistic effect at specific ratios, increasing cell death (apoptosis) and oxidative stress. This combination was more effective at slowing tumor growth compared to either compound alone. The synergy likely results from the combined action of CUR and disulfiram on the NF- $\kappa$ B and PI3K/Akt signaling pathways, which enhances apoptosis and slows cell growth.

### 3.5. Migration Test (Scratch Assay)

A Scratch Assay was performed on B16 melanoma cells over two days to assess cell migration after treatment with different concentrations of CUR-NIC and liposomal formulations. At the highest concentration of CUR-NIC (52  $\mu$ M), the scratch area stayed mostly clear by Day 2, showing strong inhibition of cell migration. At 26  $\mu$ M, migration was moderately inhibited, while at 13  $\mu$ M, some migration occurred, but it was still less than the control group (p-value <0.05). This demonstrates that CUR-NIC inhibits cell migration in a concentration-dependent manner, highlighting its potential to prevent tumor metastasis.

Similarly, Lip-CUR-NIC was tested at various concentrations over two days. Control samples showed significant cell migration by Day 2, while Lip-CUR-NIC at 100  $\mu$ M showed a strong inhibition of migration. At 50  $\mu$ M, the migration was moderate, and at 25  $\mu$ M, slight migration was observed. These results indicate that Lip-CUR-NIC can effectively block B16 melanoma cell migration in a dose-dependent manner (Figure 7A, 7B). Control bars in the figures represent the baseline migration of untreated cells, providing a point of comparison for the treated samples (Figure 7C).

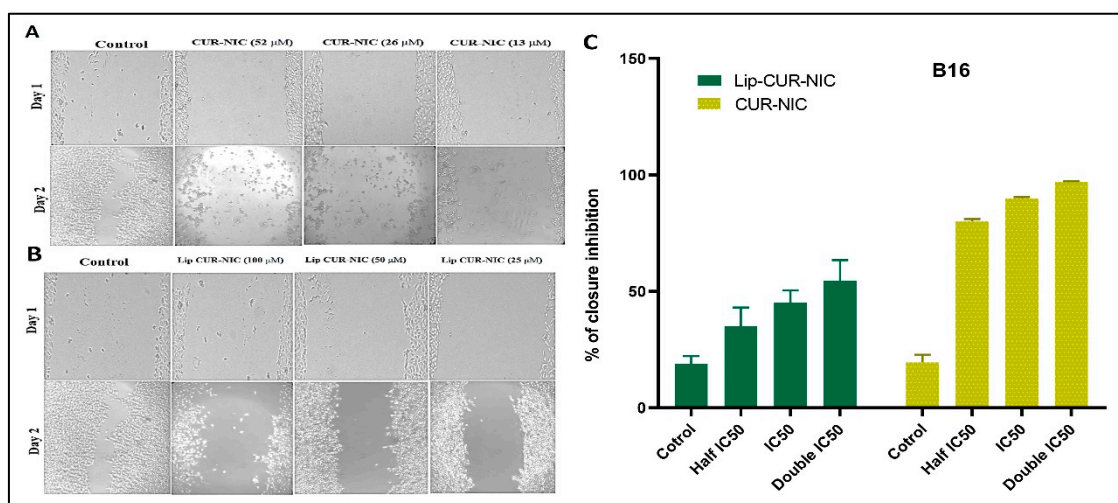


**Figure 7.** Effect of CUR-NIC and Lip-CUR-NIC on cell migration and invasion capability. (A) The migration of B16 melanoma cells in the Matrigel surface after 48 h of scrape in different concentration  $1/2 *IC_{50}$ ,  $IC_{50}$  and  $2*IC_{50}$  (26,  $2IC_{50}$  (13, 26, 52  $\mu$ M) of CUR-NIC combination groups. (B) show the migration of B16 melanoma cells in the matrigel surface after 48 h of scrape in different concentration  $1/2 *IC_{50}$ ,  $IC_{50}$  and  $2*IC_{50}$  (25, 50, 100  $\mu$ M) of Lip-CUR-NIC. (C) The cells migration inhibited distance for all the formulations and free drugs were calculated. (Quantification of the wound scratch assay shown Data are expressed as a mean  $\pm$  SD, for 24 hrs. and n=2).

The liposomal formulation may not have shown enhanced inhibition at lower concentrations due to a combination of factors like slower drug release, lower uptake by the cells, suboptimal encapsulation efficiency. Therefore, longer observation period might reveal greater efficacy for Lip-CUR-NIC, as its sustained release could take longer to show significant inhibition compared to the free drug, which is more rapidly bioavailable.

#### 4. Conclusion

In conclusion, the CUR-NIC combination exhibited significant anticancer activity, as shown by the MTT assay, indicating a synergistic effect that could offer a more effective cancer treatment strategy. The DPPH assay confirmed the antioxidant properties of the CUR-NIC combination, which may enhance its anticancer efficacy.

The ethanol injection technique was optimized for the encapsulation of CUR and NIC by adjusting parameters like the lipid-to-drug ratio, ethanol concentration, and injection rate. The main challenge was balancing CUR's hydrophobic nature and NIC's hydrophilic properties to achieve stable liposomes with high encapsulation efficiency. By fine-tuning the formulation, efficient encapsulation and stable particle size were achieved despite the differences in solubility between the two compounds.

In summary, this study presents the potential use of the CUR and NIC combination in melanoma therapy and the treatment of skin infections caused by *S. aureus*. Moreover, the results suggest that CUR, NIC, CUR-NIC, and their liposomal forms warrant further investigation as promising strategies to combat *S. aureus*. Future research should focus on in vivo studies, mechanistic investigations, combination therapies, and clinical trials to validate the effectiveness, safety, and clinical translation potential of this formulation. Future studies should aim at in vivo testing to confirm the observed benefits, optimize dosage and formulation, and ensure that these treatments are safe for human use.

#### References

1. Sorrenti, V., et al., *Recent Advances in Health Benefits of Bioactive Compounds from Food Wastes and By-Products: Biochemical Aspects*. Int J Mol Sci, 2023. 24(3).
2. Nsairat, H., et al., *Impact of nanotechnology on the oral delivery of phyto-bioactive compounds*. Food Chemistry, 2023. 424: p. 136438.
3. Lafi, Z., et al., *A review Echinomycin: A Journey of Challenges*. Jordan Journal of Pharmaceutical Sciences, 2023. 16(3): p. 640-654.
4. Hammad, H.M., et al., *Ethanol extract of Achillea fragrantissima enhances angiogenesis through stimulation of VEGF production*. Endocrine, Metabolic & Immune Disorders-Drug Targets (Formerly Current Drug Targets-Immune, Endocrine & Metabolic Disorders), 2021. 21(11): p. 2035-2042.
5. Lafi, Z.M., et al., *Association of rs7041 and rs4588 polymorphisms of the vitamin D binding protein and the rs10741657 polymorphism of CYP2R1 with vitamin D status among Jordanian patients*. Genetic testing and molecular biomarkers, 2015. 19(11): p. 629-636.
6. Watkins, R.R. and R.A. Bonomo, *Overview: Global and Local Impact of Antibiotic Resistance*. Infect Dis Clin North Am, 2016. 30(2): p. 313-322.
7. Hussain, Y., et al., *Antimicrobial Potential of Curcumin: Therapeutic Potential and Challenges to Clinical Applications*. Antibiotics (Basel), 2022. 11(3).
8. Chinemerem Nwobodo, D., et al., *Antibiotic resistance: The challenges and some emerging strategies for tackling a global menace*. J Clin Lab Anal, 2022. 36(9): p. e24655.
9. Laikova, K.V., et al., *Advances in the understanding of skin cancer: ultraviolet radiation, mutations, and antisense oligonucleotides as anticancer drugs*. Molecules, 2019. 24(8): p. 1516.
10. Abd El-Hack, M.E., et al., *The efficacy of polyphenols as an antioxidant agent: An updated review*. International Journal of Biological Macromolecules, 2023: p. 126525.
11. Munef, A., Z. Lafi, and N. Shalan, *Investigating anti-cancer activity of dual-loaded liposomes with thymoquinone and vitamin C*. Therapeutic Delivery, 2024. 15(4): p. 267-278.
12. AlSaleh, A., et al., *Synergistic antimicrobial effect of ascorbic acid and nicotinamide with rifampicin and vancomycin against SCCmec type IV methicillin-resistant Staphylococcus aureus (MRSA)*. Access Microbiol, 2023. 5(2).
13. Simmons, J.D., et al., *Nicotinamide Limits Replication of Mycobacterium tuberculosis and Bacille Calmette-Guérin Within Macrophages*. J Infect Dis, 2020. 221(6): p. 989-999.
14. Murray, M.F., *Nicotinamide: an oral antimicrobial agent with activity against both Mycobacterium tuberculosis and human immunodeficiency virus*. Clinical infectious diseases, 2003. 36(4): p. 453-460.

15. Starr, P., *Oral Nicotinamide Prevents Common Skin Cancers in High-Risk Patients, Reduces Costs*. Am Health Drug Benefits, 2015. 8(Spec Issue): p. 13-4.
16. Allen, N.C., et al., *Nicotinamide for Skin-Cancer Chemoprevention in Transplant Recipients*. New England Journal of Medicine, 2023. 388(9): p. 804-812.
17. Tosti, G., et al., *The Role of Nicotinamide as Chemo-Preventive Agent in NMSCs: A Systematic Review and Meta-Analysis*. Nutrients, 2024. 16(1): p. 100.
18. Surjana, D., G.M. Halliday, and D.L. Damian, *Role of nicotinamide in DNA damage, mutagenesis, and DNA repair*. Journal of nucleic acids, 2010. 2010.
19. Salech, F., et al., *Nicotinamide, a poly [ADP-ribose] polymerase 1 (PARP-1) inhibitor, as an adjunctive therapy for the treatment of Alzheimer's disease*. Frontiers in Aging Neuroscience, 2020. 12: p. 255.
20. Lafi, Z., T. Hiba, and A. Hanan, *An updated assessment on anticancer activity of screened medicinal plants in Jordan: Mini review*. Journal of Pharmacognosy and Phytochemistry, 2020. 9(5): p. 55-58.
21. Lafi, Z., N. Aboalhaja, and F. Afifi, *Ethnopharmacological importance of local flora in the traditional medicine of Jordan:(A mini review)*. Jordan Journal of Pharmaceutical Sciences, 2022. 15(1): p. 132-144.
22. Lafi, Z., et al., *Aptamer-functionalized pH-sensitive liposomes for a selective delivery of echinomycin into cancer cells*. RSC Advances, 2021. 11(47): p. 29164-29177.
23. Alshaer, W., et al., *Encapsulation of echinomycin in cyclodextrin inclusion complexes into liposomes: in vitro anti-proliferative and anti-invasive activity in glioblastoma*. RSC advances, 2019. 9(53): p. 30976-30988.
24. Allateef, A., N. Shalan, and Z. Lafi, *Anticancer activity of liposomal formulation co-encapsulated with coumarin and phenyl butyric acid*. Journal of Applied Pharmaceutical Science, 2024.
25. Weinstein, M.P. and J.S. Lewis, *The clinical and laboratory standards institute subcommittee on antimicrobial susceptibility testing: background, organization, functions, and processes*. Journal of clinical microbiology, 2020. 58(3): p. e01864-19.
26. Grimmig, R., et al., *Development and evaluation of a prototype scratch apparatus for wound assays adjustable to different forces and substrates*. Applied Sciences, 2019. 9(20): p. 4414.
27. De Leo, V., et al., *Encapsulation of Curcumin-Loaded Liposomes for Colonic Drug Delivery in a pH-Responsive Polymer Cluster Using a pH-Driven and Organic Solvent-Free Process*. Molecules, 2018. 23(4).
28. Zhang, Q., et al., *The mechanism of nicotinamide on reducing acute lung injury by inhibiting MAPK and NF- $\kappa$ B signal pathway*. Mol Med, 2021. 27(1): p. 115.
29. Harush-Frenkel, O., et al., *A safety and tolerability study of differently-charged nanoparticles for local pulmonary drug delivery*. Toxicology and Applied Pharmacology, 2010. 246(1): p. 83-90.
30. Shajari, M., et al., *Eco-friendly curcumin-loaded nanostructured lipid carrier as an efficient antibacterial for hospital wastewater treatment*. Environmental Technology & Innovation, 2020. 18: p. 100703.
31. Stavri, M., L.J. Piddock, and S. Gibbons, *Bacterial efflux pump inhibitors from natural sources*. J Antimicrob Chemother, 2007. 59(6): p. 1247-60.
32. Teow, S.Y. and S.A. Ali, *Synergistic antibacterial activity of Curcumin with antibiotics against Staphylococcus aureus*. Pak J Pharm Sci, 2015. 28(6): p. 2109-14.
33. Mun, S.H., et al., *Synergistic antibacterial effect of curcumin against methicillin-resistant Staphylococcus aureus*. Phytomedicine, 2013. 20(8-9): p. 714-8.
34. Zhou, Z., et al., *Combination of erythromycin and curcumin alleviates Staphylococcus aureus induced osteomyelitis in rats*. Frontiers in cellular and infection microbiology, 2017. 7: p. 379.
35. Wang, Y., et al., *Study on the antibiotic activity of microcapsule curcumin against foodborne pathogens*. Int J Food Microbiol, 2009. 136(1): p. 71-4.
36. Gunes, H., et al., *Antibacterial effects of curcumin: An in vitro minimum inhibitory concentration study*. Toxicol Ind Health, 2016. 32(2): p. 246-50.
37. Shailendiran, D., et al. *Characterization and Antimicrobial Activity of Nanocurcumin and Curcumin*. in 2011 International Conference on Nanoscience, Technology and Societal Implications. 2011.
38. Hu, P., P. Huang, and M.W. Chen, *Curcumin reduces Streptococcus mutans biofilm formation by inhibiting sortase A activity*. Arch Oral Biol, 2013. 58(10): p. 1343-8.
39. Izui, S., et al., *Antibacterial Activity of Curcumin Against Periodontopathic Bacteria*. J Periodontol, 2016. 87(1): p. 83-90.

**Disclaimer/Publisher's Note:** The statements, opinions and data contained in all publications are solely those of the individual author(s) and contributor(s) and not of MDPI and/or the editor(s). MDPI and/or the editor(s) disclaim responsibility for any injury to people or property resulting from any ideas, methods, instructions or products referred to in the content.